Studies of *aberrant phyllotaxy1* Mutants of Maize Indicate Complex Interactions between Auxin and Cytokinin Signaling in the Shoot Apical Meristem[1][W][OA]

Byeong-ha Lee[2], Robyn Johnston[2], Yan Yang, Andrea Gallavotti, Mikiko Kojima, Bruno A.N. Travençolo, Luciano da F. Costa, Hitoshi Sakakibara, and David Jackson*

Cold Spring Harbor Laboratory, Cold Spring Harbor, New York 11724 (B.-h.L., R.J., Y.Y., A.G., D.J.); Department of Life Science, Sogang University, Seoul 121–742, Korea (B.-h.L.); University of Amsterdam, Amsterdam, 1098SM, The Netherlands (Y.Y.); Section of Cell and Development Biology, University of California, San Diego, La Jolla, California 92093–0116 (A.G.); Plant Science Center, RIKEN, Tsurumi, Yokohama 230–0045, Japan (M.K., H.S.); and Instituto de Física de São Carlos, Universidade de São Paulo, São Carlos, São Paulo 13560–970, Brazil (B.A.N.T., L.d.F.C.)

One of the most fascinating aspects of plant morphology is the regular geometric arrangement of leaves and flowers, called phyllotaxy. The shoot apical meristem (SAM) determines these patterns, which vary depending on species and developmental stage. Auxin acts as an instructive signal in leaf initiation, and its transport has been implicated in phyllotaxy regulation in Arabidopsis (*Arabidopsis thaliana*). Altered phyllotactic patterns are observed in a maize (*Zea mays*) mutant, *aberrant phyllotaxy1* (*abph1*, also known as *abphyl1*), and *ABPH1* encodes a cytokinin-inducible type A response regulator, suggesting that cytokinin signals are also involved in the mechanism by which phyllotactic patterns are established. Therefore, we investigated the interaction between auxin and cytokinin signaling in phyllotaxy. Treatment of maize shoots with a polar auxin transport inhibitor, 1-naphthylphthalamic acid, strongly reduced *ABPH1* expression, suggesting that auxin or its polar transport is required for *ABPH1* expression. Immunolocalization of the PINFORMED1 (PIN1) polar auxin transporter revealed that PIN1 expression marks leaf primordia in maize, similarly to Arabidopsis. Interestingly, maize PIN1 expression at the incipient leaf primordium was greatly reduced in *abph1* mutants. Consistently, auxin levels were reduced in *abph1*, and the maize PIN1 homolog was induced not only by auxin but also by cytokinin treatments. Our results indicate distinct roles for *ABPH1* as a negative regulator of SAM size and a positive regulator of PIN1 expression. These studies highlight a complex interaction between auxin and cytokinin signaling in the specification of phyllotactic patterns and suggest an alternative model for the generation of altered phyllotactic patterns in *abph1* mutants. We propose that reduced auxin levels and PIN1 expression in *abph1* mutant SAMs delay leaf initiation, contributing to the enlarged SAM and altered phyllotaxy of these mutants.

The shoot apical meristem (SAM) initiates lateral organs and determines their regular geometric spacing, or phyllotaxy. Different phyllotactic patterns are characteristic of specific species or developmental stages and include alternate, opposite and decussate, whorled, and spiral patterns. Although it has long drawn attention from biologists and mathematicians, until recently the molecular mechanism behind the generation of these fascinating patterns was not well understood. Molecular developmental studies suggest a phyllotaxy regulation model based on polar auxin transport by the PINFORMED1 (PIN1) auxin efflux carrier (Reinhardt et al., 2003; Petrasek et al., 2006; Wisniewska et al., 2006). Inhibition of polar auxin transport or mutations in the PIN1 auxin efflux carrier disrupt leaf or flower initiation in tomato (*Solanum lycopersicum*), Arabidopsis (*Arabidopsis thaliana*), and maize (*Zea mays*; Okada et al., 1991; Reinhardt et al., 2000; Scanlon, 2003). When auxin was applied locally to these pin-like SAMs, lateral organ outgrowth was restored at the application site. In Arabidopsis, PIN1-regulated polar auxin transport plays a crucial role in lateral organ positioning and initiation (Benkova et al., 2003; Reinhardt et al., 2003). PIN1 protein is expressed throughout the L1 layer of the SAM, and near the leaf initiation sites, its polar localization is directed toward the initiation sites (Reinhardt et al., 2003). As the subcellular localization of PIN directs the flow of

[1] This work was supported by the Conselho Nacional de Desenvolvimento Científico e Tecnológico (grant no. 308231/03–1 to L.d.F.C.), by the Fundação de Amparo à Pesquisa do Estado de São Paulo (grant no. 03/13072–8 to B.A.N.T.), by a Cold Spring Harbor Laboratory association fellowship to A.G., by a Special Research Grant of Sogang University to B.-h.L., and by the National Science Foundation (grant no. IOB 0642707 to B.-h.L., R.J., and D.J. and grant no. DBI–0501862 to Y.Y. and D.J.).

[2] These authors contributed equally to the article.

* Corresponding author; e-mail jacksond@cshl.edu.

The author responsible for distribution of materials integral to the findings presented in this article in accordance with the policy described in the Instructions for Authors (www.plantphysiol.org) is: David Jackson (jacksond@cshl.edu).

[W] The online version of this article contains Web-only data.

[OA] Open Access articles can be viewed online without a subscription.

www.plantphysiol.org/cgi/doi/10.1104/pp.109.137034

auxin (Wisniewska et al., 2006), the hormone is transported in the L1 layer to leaf initiation sites, where auxin maxima are formed. Subsequently, the PIN1 expression domain extends inward to form a provascular stream toward the vascular tissues in the stem. These cells drain auxin away from the leaf primordium, causing depletion of auxin in the surrounding area. As a result of this sink, only regions distant from existing primordia are able to accumulate auxin and initiate new primordia. This model, therefore, explains the spacing component of phyllotaxy, but not how the patterns arise de novo. From these basic principles, several computational models of phyllotaxy have been developed (de Reuille et al., 2006; Jonsson et al., 2006; Smith et al., 2006). Despite the strong implication of auxin in phyllotaxy regulation, no auxin mutants in Arabidopsis display obvious changes in their phyllotactic pattern.

One of the very few mutants known to specifically affect phyllotaxy maps to the *ABERRANT PHYLLOTAXY1* (*ABPH1*) locus in maize (Giulini et al., 2004). *abph1* mutants develop decussate phyllotaxy, in which leaves are paired at 180°, whereas normal maize plants have a distichous phyllotaxy, with leaves developing in an alternating pattern (Jackson and Hake, 1999). *ABPH1* encodes a cytokinin-inducible type A response regulator, suggesting that cytokinin signals are important for phyllotaxy regulation in maize (Giulini et al., 2004). Cytokinin signaling occurs through a two-component signaling pathway, involving a phosphorylation cascade from His kinase receptors at the cell surface to nuclear response regulators (Hwang and Sheen, 2001). The general importance of cytokinin signaling in the SAM is well established. Cytokinin overproduction results in increased transcript levels of *KNOTTED-LIKE1* (*KNAT1*) and *SHOOTMERISTEMLESS* (*STM*), genes that are involved in the regulation of SAM function, while cytokinin-deficient plants or triple cytokinin receptor knockout mutants show reduced SAM development (Rupp et al., 1999; Werner et al., 2001, 2003; Higuchi et al., 2004; Nishimura et al., 2004). Cytokinins also appear to regulate the maintenance of a stem cell population in the SAM via a feedback loop between *CLAVATA3* and *WUSCHEL* (*WUS*) genes (Brand et al., 2000; Schoof et al., 2000; Spradling et al., 2001; Weigel and Jurgens, 2002; Laux, 2003). Recently, *WUS* was shown to directly repress several cytokinin-inducible type A response regulators in the SAM (Leibfried et al., 2005). This result directly connects stem cell maintenance in the SAM to cytokinin signaling.

Auxins and cytokinins function together in many plant developmental processes. One classical example is in vitro plant culture, where commitment to shoot or root development is determined by the ratio of these hormones (Skoog and Miller, 1957). We hypothesized previously that the change in phyllotaxy in *abph1* mutants results from a cytokinin-dependent increase in SAM size, which creates more available space for leaf initiation. However the observation that *ABPH1* expression in the seedling SAM overlaps with the "plastochron zero" (P_0) domain of leaf initiation suggests an alternative hypothesis that invokes a role for ABPH1 in the regulation of leaf initiation. This hypothesis is attractive in light of the fact that auxin transport by *PIN1* functions in Arabidopsis phyllotaxy, and cytokinin regulation by *ABPH1* in maize phyllotaxy, and suggests that these differences are not species specific but that cross talk between auxin and cytokinin signaling may be important in phyllotaxy regulation in diverse plant species. This hypothesis is supported by the observation that in maize both *PIN1* and *ABPH1* are expressed in what appear to be overlapping domains at the leaf initiation site or P_0 (Giulini et al., 2004; Carraro et al., 2006). Cytokinins and auxins also appear to coordinately regulate root development. Cytokinins disrupt the formation of auxin maxima during Arabidopsis lateral root development by reducing the expression levels of *PIN* genes (Laplaze et al., 2007). Auxin-cytokinin cross talk also regulates development of the Arabidopsis root apical meristem (Dello Ioio et al., 2007) and the establishment of the embryonic root apical meristem (Müller and Sheen, 2008). Therefore, we investigated interactions between cytokinin and auxin signaling in the control of phyllotaxy in maize.

Here, we show that treatment with the polar auxin transport inhibitor 1-naphthylphthalamic acid (NPA) greatly reduced the expression of *ABPH1*, suggesting that *ABPH1* expression is dependent on the accumulation of auxin at incipient leaf primordia. Surprisingly, we also found that maize *PIN1* expression was strongly reduced in *abph1* mutant meristems, indicating that *ABPH1* is required for normal expression of *PIN1*. In addition, *abph1* mutant embryos had lower concentrations of auxin compared with normal embryos, supporting the idea that *ABPH1* is important for auxin accumulation. Taken together, these results imply a positive feedback loop involving polar auxin transport and maize *PIN1*, and *ABPH1* expression at incipient leaf primordia. Therefore, *ABPH1* acts both as a positive regulator of auxin levels and PIN1 signaling (this study) and as a negative regulator in cytokinin signaling in SAM size determination (Giulini et al., 2004). We propose that the reduced levels of PIN1 expression in *abph1* shoot meristems may explain the observed delay in leaf initiation in *abph1* mutants, which suggests an alternative model to explain the altered phyllotaxy in *abph1* mutants.

RESULTS

ABPH1 Expression Is Reduced following NPA Treatment

abph1 mutants initiate leaves in an altered phyllotaxy, in opposite pairs, in contrast to the normal alternate pattern in maize. During seedling development, *ABPH1* is expressed in the leaf initiation site (P_0) of the maize SAM, suggesting that it plays a role in leaf

positioning (Fig. 1A; Giulini et al., 2004). As polar auxin transport and local auxin accumulation at the leaf initiation site are required for leaf initiation in Arabidopsis and maize (Reinhardt et al., 2003; Scanlon, 2003; Carraro et al., 2006), we examined *ABPH1* expression after treatment with the polar auxin transport inhibitor NPA. Two-week-old shoot apices were cultured on control Murashige and Skoog (MS) medium or on medium with 30 μM NPA, as described (Scanlon, 2003). Apices were then fixed and subjected to in situ hybridization. While the expected *ABPH1* expression domain (Giulini et al., 2004) was detected in the P_0 or incipient leaf primordium in the control apices without NPA treatment (Fig. 1A), *ABPH1* expression was absent (Fig. 1, B and C) or reduced and confined to the L1 layer of incipient leaf primordia (Fig. 1D) in apices treated with NPA for 5 to 14 d. Similar results were found in more than 12 treated apices.

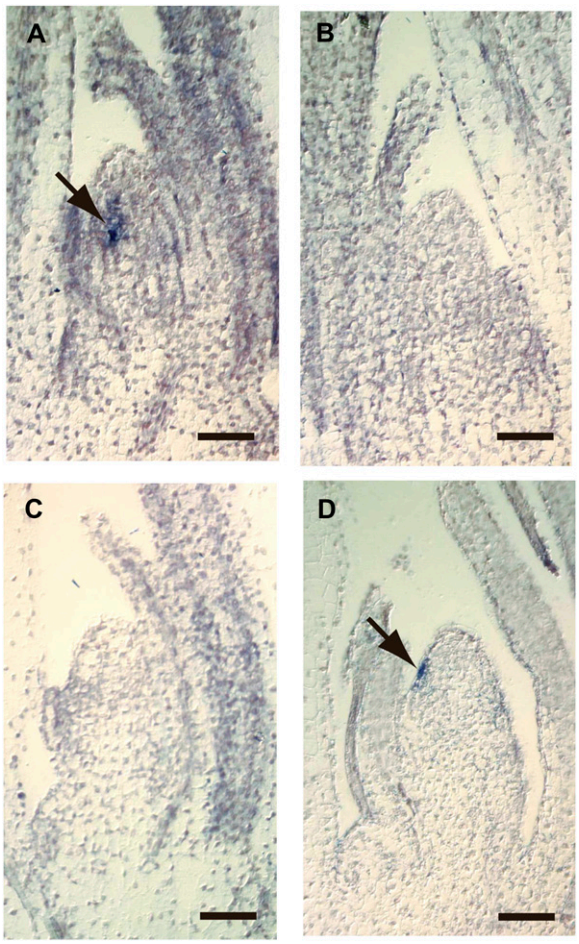

Figure 1. NPA treatment inhibits *ABPH1* expression in the SAM. Longitudinal sections of maize shoot apices processed for *ABPH1* in situ hybridization. Two-week-old maize seedlings were grown on MS medium without NPA for 10 d (A) or with 30 μM NPA for 5 d (B), 10 d (C), or 14 d (D). Arrows indicate *ABPH1* expression (A) and residual weak expression (D). Bars = 100 μm.

To ask if this effect was likely to be due to a direct effect of auxin signaling or a downstream consequence of blocking leaf initiation by NPA treatment, we measured *ABPH1* expression following shorter NPA treatments. After a 24-h treatment with NPA, we found no significant difference in *ABPH1* expression in the SAMs of treated and control plants (*ABPH1* levels were normalized relative to ubiquitin expression, and signal intensity in control treatments was arbitrarily set to 1; treated plants had a signal intensity of 0.96 $\pm$ 0.20 for the treated samples). As a control to confirm that a 24-h treatment with NPA is sufficient to affect auxin transport in the SAM, we measured *ZmPIN1a* expression in the SAMs of NPA-treated and control plants. We found that *ZmPIN1a* expression was increased in the SAMs of NPA-treated seedlings compared with control seedlings (*ZmPIN1a* levels were normalized relative to ubiquitin expression, and signal intensity in control treatments was arbitrarily set to 1; treated plants had a signal intensity of 2.90 $\pm$ 0.19). This observation is consistent with a previous report that enhanced expression of the auxin-responsive DR5 promoter-GFP reporter was observed in the Arabidopsis SAM after short-term NPA treatment (Benkova et al., 2003). Our result serves as a control to show that NPA influences auxin dynamics in the maize SAM within 24 h. The finding that 24 h of treatment with NPA does not alter *ABPH1* expression suggests that the reduction in *ABPH1* expression seen in SAMs treated for several days with NPA is unlikely to be a direct effect of reduced auxin transport and may be downstream of the block in leaf initiation. Therefore, the expression of *ABPH1* is dependent on polar auxin transport, but this response is likely to be indirect.

An Arabidopsis PIN1 Antiserum Detects Maize PIN1 Expression

Here, we used an Arabidopsis PIN1 antiserum raised against a peptide (GPTPRPSNYEEDGGPA) located in the Gly-rich domain of the large intracellular loop of PIN1, which has previously been used to detect PIN1 proteins in Arabidopsis, maize, and *Medicago* (Boutte et al., 2006; Carraro et al., 2006; de Reuille et al., 2006). This antiserum detects PIN1 localization in the Arabidopsis SAM in the same pattern as in other studies using different PIN1 antisera or GFP fusions (Benkova et al., 2003; Reinhardt et al., 2003; Heisler et al., 2005; de Reuille et al., 2006). We first tested the specificity of the antiserum using maize protein extracts from shoot apices. A western blot detected a band of similar size (approximately 65 kD) to the predicted maize PIN1 proteins (see below; Supplemental Fig. S1). The band was weak in the soluble fraction and strong in the membrane fraction, as predicted for a membrane-localized protein.

An earlier report (Carraro et al., 2006) suggested that the pattern of PIN1 expression in maize was different, as they did not detect prominent PIN1 expression in the L1 layer like the reported expression

in Arabidopsis. Here, we detected significant L1 expression of maize PIN1, and our results are described in detail below.

The Maize PIN1 Expression Pattern in the SAM Is Similar to That in Arabidopsis

In Arabidopsis, PIN1 is preferentially expressed throughout the epidermis (L1 layer) of the SAM and, in most cells, is localized to the side of the cell that is nearest the tip of the SAM (Reinhardt et al., 2003). However, in cells near the incipient leaf primordium (P_0), PIN1 is localized toward the P_0, suggesting that auxin is transported in the L1 toward the P_0 (Reinhardt et al., 2003). Immunolocalization with maize shoot apices also revealed polar localization patterns in the SAM (Fig. 2). Therefore, the Arabidopsis PIN1 antiserum appears able to detect maize PIN1 proteins in situ. In the maize SAM, PIN1 was not expressed strongly throughout the L1 layer but accumulated preferentially in epidermal cells near the P_0 (Fig. 2, A and B). In epidermal cells that expressed maize PIN1, the protein was preferentially localized to the side of the cell nearest the P_0, similar to the pattern described in Arabidopsis (Fig. 2B). Therefore, it appears likely that auxin is transported in the L1 toward the P_0 in maize, as in Arabidopsis.

We also observed that maize PIN1 expression extended inward from the P_0 and young leaf primordia, presumably marking the provascular strands (Fig. 2, A and B). In these cells, the protein was polarly localized downward and toward the center of the shoot apex in two to three cell files. These cell files merged in the center of the stem (Fig. 2A). These patterns are also similar to those seen in Arabidopsis (Reinhardt et al., 2003). Thus, as proposed in Arabidopsis, the inward PIN1 localization from the P_0 and young leaf primordia likely serves to form auxin sinks to deplete auxin close to existing primordia. Interestingly, we also observed an additional domain of maize PIN1 expression in the center of the SAM (Fig. 2A), as reported previously (Carraro et al., 2006). The importance of this domain is unknown, but it may be significant because PIN1 was also polarly localized within these cells.

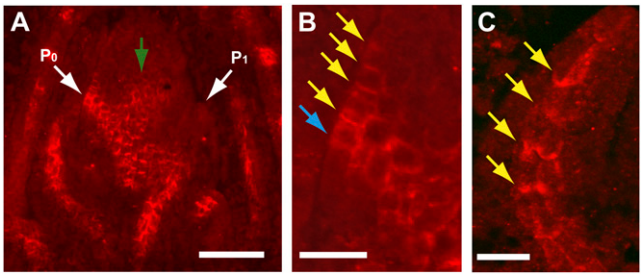

Figure 2. Maize PIN1 is detected by an Arabidopsis PIN1 antiserum. A, Maize PIN1 immunolocalization in normal maize SAM. P_0 and P_1 leaf primordia are indicated with white arrows. The green arrow shows the maize PIN1 expression domain in the center of the SAM. Bar = 100 μm. B, Magnified incipient leaf initiation site (P_0). Yellow arrows indicate basal localization of maize PIN1, and the blue arrow indicates apical localization of maize PIN1 in the L1 epidermal cells. Bar = 30 μm. C, Basal localization of maize PIN1 in provascular cells of a P_1 leaf primordium. Yellow arrows show the basal localization of maize PIN1 protein. Bar = 25 μm.

Immunolocalization Shows That Maize PIN1 Expression Is Strongly Reduced in *abph1* Plants

To investigate how PIN1 signaling might be affected in the *abph1* phyllotaxy mutant, we also performed immunolocalization in the mutant background. As in normal maize shoot apices, PIN1 expression marked young leaf primordia in *abph1*, suggesting that the auxin sink function in these young primordia is not affected in *abph1* mutants (Fig. 3A). However, the PIN1 expression that normally marks the P_0 site was absent or very weak in *abph1* (Fig. 3, B–E). As the P_0 should be located at 90° to the P_1 in *abph1*, rather than opposite as in the wild type, longitudinal median sections might miss the P_0. Thus, we carried out immunolocalizations using transverse sections of *abph1* apices and found the same results (Fig. 3, F and G). In *abph1* mutants, leaf initiation itself is not defective, and older *abph1* leaf primordia have normal PIN1 expression (Fig. 3, A and G); therefore, we interpret the weak expression in the P_0 as a delay in the onset of PIN1 expression in *abph1* mutants. We also observed maize PIN1 expression in a small domain in the center of the *abph1* SAM, as seen in the wild type (Fig. 3A).

To confirm the changes in maize PIN1 expression, we performed three-dimensional (3D) image reconstruction of a series of longitudinal immunolocalization sections. These reconstructions confirmed the maize PIN1 expression domains associated with leaf primordia (Fig. 3, H and I; Supplemental Videos S1 and S2) and again indicated clearly that PIN1 expression was absent from the P_0 positions in *abph1*.

A Maize PIN1 Homolog Is Auxin Inducible in the SAM and Is Down-Regulated in *abph1* Mutants

To determine whether our findings with the cross-reacting Arabidopsis PIN1 antiserum were also true for the endogenous maize *PIN1* gene, and if regulation by *ABPH1* might be at the transcriptional level, we identified maize *PIN1* homologs. We screened a maize bacterial artificial chromosome (BAC) library (NSF B73; Clemson University Genomics Institute) using the first predicted exon sequence of the maize gene most similar to PIN1 (AZM5_9949; http://maize.tigr.org/). We identified two overlapping BAC clones and sequenced approximately 10 kb of genomic sequence of the locus, which we named *ZmPIN1*. This sequence corresponds to *ZmPIN1a*, as also described by Carraro et al. (2006). Shoot meristem-enriched cDNA libraries from immature ears and tassels were screened for

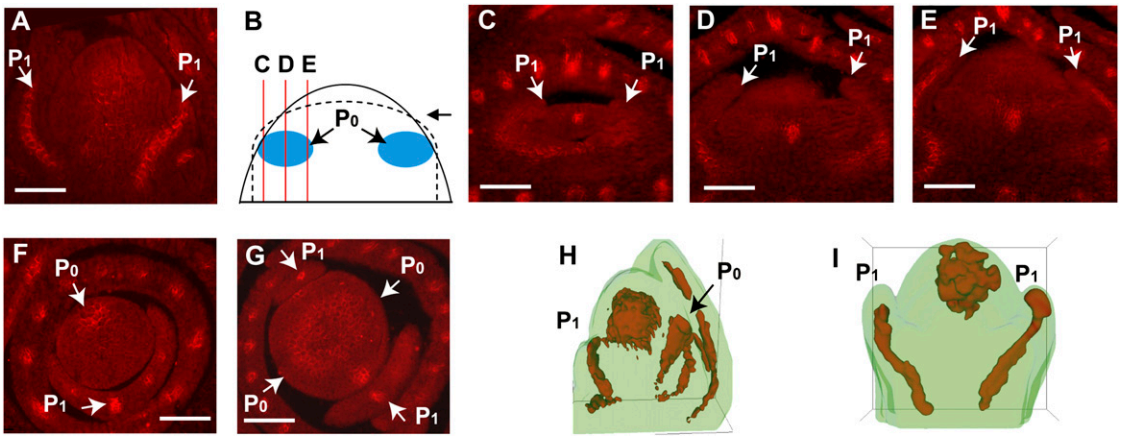

Figure 3. Immunolocalization reveals PIN1 expression differences in *abph1* mutants. A, Immunolocalization of PIN1 in *abph1* SAM showing normal expression at P_1 (arrows). B, Diagram to show the positions of longitudinal sections in C to E. The solid line indicates the SAM. The dotted line indicates the newly initiated (P_1) leaf primordia. Red lines indicate sectioning planes. Letters correspond to each labeled panel. The arrow indicates the view point. P_0 is labeled in blue. C to E, PIN1 immunolocalization in serial sections of the *abph1* shoot apex. Bright signal in the center indicates provascular development. Arrows indicate P_1. Note the lack of PIN1 expression in the presumed P_0 position. F and G, PIN1 immunolocalization in transverse sections of normal (F) and *abph1* (G) shoot apices. Arrows indicate each leaf position, as labeled. Note that the plane of the section in G is not precisely horizontal, hence the two P1 primordia appear slightly different sizes. Note the lack of PIN1 expression in the presumed P_0 position. H and I, 3D reconstructions of PIN1 immunolocalization in normal maize (H) and *abph1* (I) shoot apices. Arrows indicate each leaf primordium, as labeled. Bars = 100 μm.

maize *PIN1* cDNAs, using the same probe used for BAC library screening. Seven clones were identified, and all of them corresponded exactly to the *ZmPIN1a* genomic clones. Comparison between *ZmPIN1a* genomic DNA and cDNA sequences revealed five introns, as in Arabidopsis *PIN1*.

To determine if *ZmPIN1a* is functionally related to Arabidopsis *PIN1*, we first examined if it was expressed in the maize SAM. Using reverse transcription (RT)-PCR, we could indeed detect *ZmPIN1a* transcripts in RNA from dissected maize SAMs (data not shown). Another property of Arabidopsis *PIN1* is its rapid induction by auxin (Heisler et al., 2005). To establish if *ZmPIN1a* is similarly induced, we performed semiquantitative RT-PCR using total RNA from 2-week-old maize apices treated with the auxin indole-3-acetic acid (IAA) for 1 h. This short treatment increased *ZmPIN1a* transcript levels significantly (Fig. 4A). In summary, *ZmPIN1a* is a maize homolog of Arabidopsis *PIN1*, and it is functionally related by its localization and auxin inducibility.

To investigate if *ZmPIN1a* is regulated by *ABPH1*, as predicted by our immunolocalization results, we performed semiquantitative RT-PCR. Meristems from normal and *abph1* seedlings were exposed by removing leaf primordia and then excised above the point of insertion of the P1 primordia, and total RNA was extracted. Semiquantitative RT-PCR results confirmed that *ZmPIN1a* transcript levels were significantly reduced in *abph1* mutant meristems (Fig. 4B). These results are consistent with the reduced PIN1 expression detected by immunolocalization in *abph1* mutants and suggest that this regulation of *ZmPIN1a* occurs at least in part at the transcriptional level.

Spatial Expression of ZmPIN1a-YFP Is Altered in *abph1* Mutant Embryos

Since we observed reduced PIN1 expression in seedlings, we also investigated whether PIN1 expression was altered in *abph1* embryos prior to leaf initiation. We used confocal microscopy to examine the expression of ZmPIN1a-yellow fluorescent protein (ZmPIN1a-YFP; Gallavotti et al., 2008) in embryos 11 to 14 d after pollination (Fig. 4, C–I). We found that ZmPIN1a-YFP expression was significantly weaker in the SAMs of *abph1* embryos compared with the wild type. In wild-type embryos, ZmPIN1a-YFP was observed in the center and lower regions of the initiating SAM prior to initiation of the first leaf (Fig. 4C). A corresponding expression domain was never observed in the SAM of *abph1* embryos (Fig. 4D). During the course of these observations, we also noticed that leaf initiation was delayed in *abph1* embryos. Embryos were staged by observation of morphological landmarks, such as the appearance of the SAM, the coleoptilar ridge, or the first leaf primordium. We estimated that this delay was approximately 1 d. We also checked older *abph1* embryos for ZmPIN1a-YFP expression. However, ZmPIN1a-YFP expression was never observed in the *abph1* embryo SAM prior to leaf emergence. As in seedlings, ZmPIN1a-YFP was expressed in *abph1* mutants in the provasculature of the first pair of leaf primordia after their initiation.

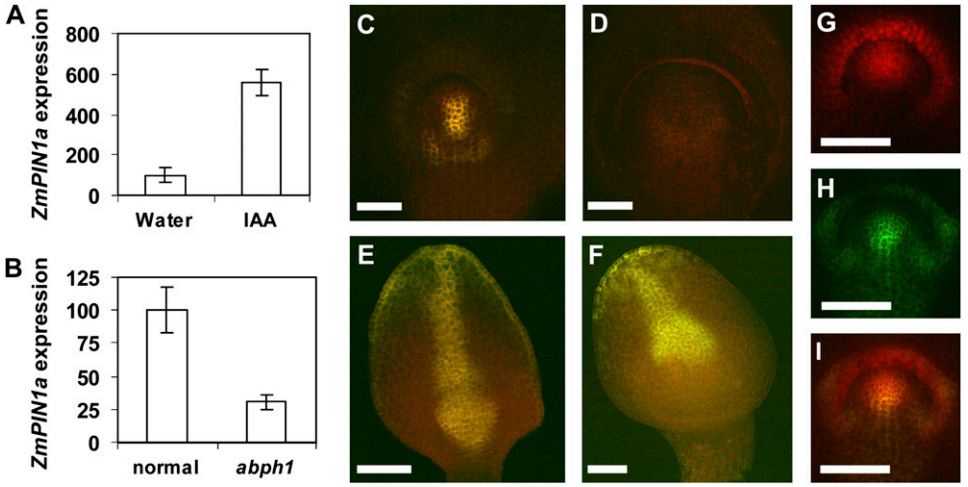

Figure 4. *ZmPIN1a* is auxin induced, and its expression is reduced in *abph1* seedlings and embryos. A, Quantification of *ZmPIN1a* expression by semiquantitative RT-PCR in shoot apices of seedlings treated with 100 μM IAA for 1 h. Expression levels (arbitrary units) were normalized based on ubiquitin expression levels, and control was adjusted to 100. Error bars indicate SE (n = 3). B, Quantification by semiquantitative RT-PCR of *ZmPIN1a* expression levels in normal and *abph1* SAMs. Expression levels (arbitrary units) were normalized based on ubiquitin expression levels. Levels of normal sample were arbitrarily adjusted to 100. Error bars indicate SE (n = 3). C, ZmPIN1a-YFP expression in a normal embryo 11 d after pollination. The strongest ZmPIN1a-YFP expression is in the central and lower parts of the SAM. PIN1 is also expressed in the emerging coleoptile. D, An *abph1* embryo 12 d after pollination. The embryo has an enlarged SAM, but no ZmPIN1a-YFP expression is visible. E, Deeper optical section through the scutellum of the normal embryo shown in C. F, Deeper optical section through the scutellum of the *abph1* embryo. G, ABPH1-RFP expression in a normal embryo 11 d after pollination. Expression is seen in the upper part of the SAM and in the coleoptile. H, ZmPIN1a-YFP expression in the normal embryo shown in G. I, Colocalization of ABPH1-RFP and ZmPIN1a-YFP in the normal embryo shown in G and H. Bars = 100 μm.

We also observed ZmPIN1a-YFP expression in deeper optical sections through the scutellum of both wild-type and *abph1* embryos (Fig. 4, E and F). The expression patterns and levels of expression in the scutellum were similar in both backgrounds, indicating that the alterations in ZmPIN1a-YFP expression were specific to the SAM and that the *abph1* embryos we observed were expressing the ZmPIN1a-YFP construct. Strong ZmPIN1a-YFP expression was observed in a patch beneath the SAM and in a central strand, presumably vasculature, that extended to the tip of the scutellum. ZmPIN1a-YFP expression was also seen at the upper edge of the scutellum.

ZmPIN1a-YFP and ABPH1-RFP Are Expressed in Partially Overlapping Domains in the Embryo SAM

Given the apparent effect of *ABPH1* on PIN1 expression, we looked more closely to determine if their expression colocalized in the embryo during SAM initiation. (Fig. 4, G–I). We imaged embryos that were expressing ZmPIN1a-YFP and an ABPH1-red fluorescent protein (ABPH1-RFP) transgene that was also driven by its native regulatory elements. We found that these proteins were indeed expressed in partially overlapping domains in the embryo SAM. ABPH1-RFP was expressed in the upper part of the SAM and in the emerging coleoptile (Fig. 4G), in a pattern similar to that seen by in situ hybridization (Giulini et al., 2004). ZmPIN1a-YFP was expressed most strongly in the central and lower parts of the SAM (Fig. 4H). The domains of ZmPIN1a-YFP and ABPH1-RFP expression overlapped in the center of the SAM (Fig. 4I).

abph1 Mutant Embryos Have a Reduced Auxin Content

The decreased levels of *ZmPIN1a* expression in *abph1* SAMs prompted us to ask whether auxin levels were altered in the mutant. In order to compare hormone levels, we used embryos similar to those shown in Figure 4 that had just started to initiate their first leaf primordia. This stage is enriched for SAM tissue (Jackson and Hake, 1999) and is preferred over isolated maize SAMs because they are too small for auxin quantification (H. Sakakibara, personal communication). *ABPH1* is expressed specifically in the SAM region in the embryo (Giulini et al., 2004); therefore, the contributions of the *abph1* mutation to the auxin differences should be mainly from the SAM, rather than from other regions of the embryo.

We found that the level of IAA was significantly lower in *abph1* mutant embryos compared with normal siblings (Fig. 5A; Supplemental Table S1). The IAA conjugate, indole-3-acetyl aspartic acid (IAAsp), was also reduced in *abph1* (Fig. 5A). The level of IAAsp is usually correlated with the levels of IAA (Ostin et al., 1998; Barratt et al., 1999; Barlier et al., 2000), consistent with the reduced IAA levels in *abph1*. Thus, the levels

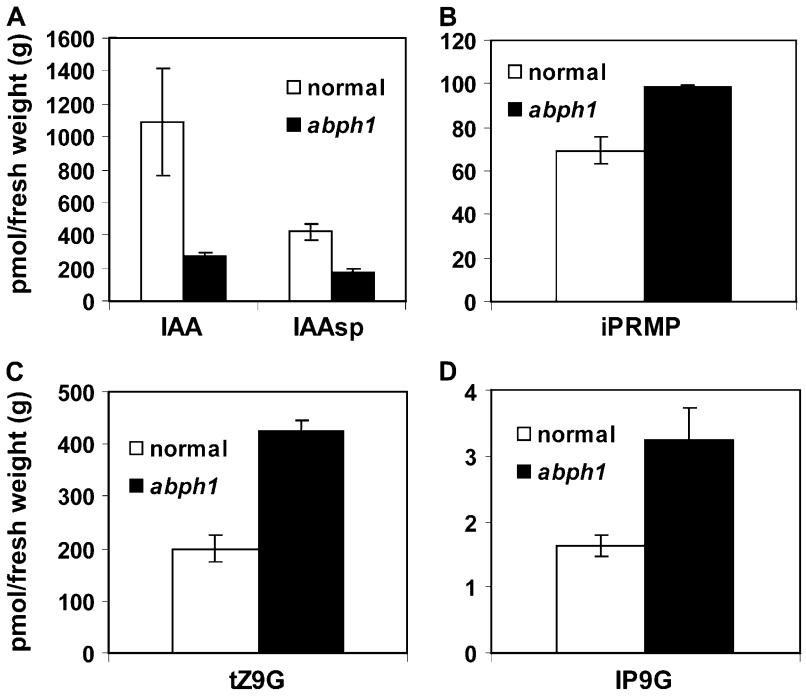

Figure 5. Hormone and hormone conjugate levels are altered in *abph1* mutants. Hormone and hormone conjugates that showed significant differences between normal maize and *abph1* are plotted. A, IAA and IAAsp. B, N^6-(Δ^2-Isopentenyl)adenine riboside 5′-monophosphate (iPRMP). C, Trans-zeatin-N^9-glucoside (tZ9G). D, Isopentenyladenine-N^9-glucoside (IP9G). Averages were calculated from three independent biological pools of approximately 10 embryos. Error bars indicate SE.

of IAA and an IAA conjugate were lower in *abph1* embryos, a finding that is consistent with the reduced *ZmPIN1a* expression in the *abph1* SAM.

We also analyzed cytokinin levels in *abph1*. Among the active cytokinins analyzed, cis-zeatin, dihydrozeatin, and N^6-(Δ^2-isopentenyl)adenine were below the detection limit and trans-zeatin did not display any significant difference. However, some cytokinin intermediates, such as N^6-(Δ^2-isopentenyl)adenine riboside 5′-monophosphate, and the inactivation reaction products isopentenyladenine-N^9-glucoside and trans-zeatin-N^9-glucoside levels were substantially increased in *abph1* mutants (Fig. 5, B–D; Supplemental Table S1). These changes could reflect local alterations in cytokinin levels in *abph1* mutants; however, this speculation is limited by our inability to measure cytokinins from very small tissue sources.

ZmPIN1a Is Rapidly Induced by Cytokinin

Since *ABPH1* was required for normal PIN1 expression in the P_0 of the SAM and *ABPH1* is rapidly induced by cytokinin (Giulini et al., 2004), we asked if *PIN1* expression was also regulated by cytokinins. We measured *ZmPIN1a* expression using semiquantitative RT-PCR of total RNA from dissected meristems. Indeed, following 1 h of treatment, *ZmPIN1a* expression was higher in the treated sample than in the water control, and a prolonged cytokinin treatment (4 h) showed further induction of *ZmPIN1a* in the cytokinin-treated SAM compared with the control (Fig. 6A). We also asked if the cytokinin induction of *ZmPIN1a* expression was altered in the *abph1* mutant. As already shown, *ZmPIN1a* expression in untreated meristems was significantly lower in *abph1* than in the wild type (Fig. 6B). However, cytokinin treatment induced *ZmPIN1a* expression to similar levels in *abph1* and normal seedlings, suggesting that *ZmPIN1a* sensitivity to cytokinin is independent of *abph1* (Fig. 6B).

To determine if cytokinin treatment alters the level of *ZmPIN1a* expression throughout the SAM, or if the increased expression is limited to the P_0, we imaged ZmPIN1a-YFP expression in the SAMs of cytokinin-treated and control plants (Fig. 6, C and D; Supplemental Fig. S3). We found that the fluorescence intensity in the P_0 was greater in cytokinin-treated than in untreated plants (Fig. 6, C and D; Supplemental Table S2; Supplemental Fig. S3). When fluorescence intensity in the entire P_0 was compared, control plants had a mean fluorescence intensity of 48 (SE = 3), whereas treated plants had a mean value of 57 (SE = 5) on a scale of 0 to 255. Measurements of fluorescence intensity in a set area of the P_0 gave similar results. The mean area of ZmPIN1a-YFP-expressing cells also increased in cytokinin-treated plants from 579 μm^2 (SE = 31) to 703 μm^2 (SE = 33). We also calculated integrated density values (defined as the product of mean fluorescence intensity and area) in the P_0 of control and treated plants as 27,143 (SE = 2,009) and 40,344 (SE = 4,156), respectively. ZmPIN1a-YFP expression in other regions of the SAM did not show a significant difference. These results indicate that cytokinin treatment specifically promotes expression of ZmPIN1a in the incipient leaf primordium.

In summary, we found a mutual requirement of auxin transport for *ABPH1* expression and *ABPH1* for *ZmPIN1a* expression, a finding that is consistent with reduced auxin levels in *abph1* mutants. *ZmPIN1a*

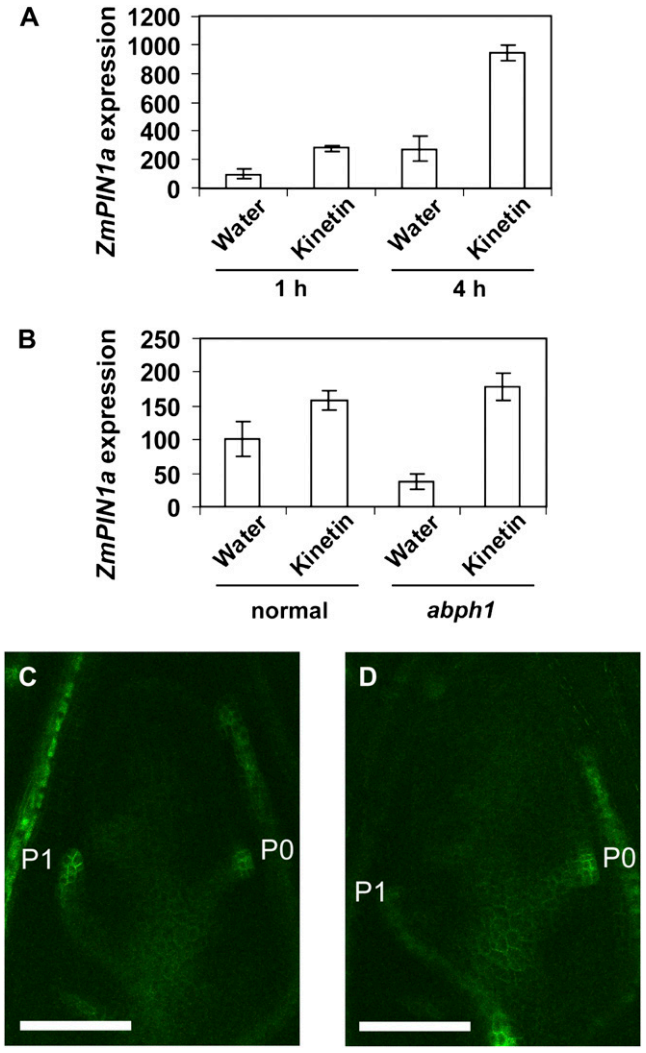

Figure 6. *ZmPIN1a* expression is rapidly induced by cytokinin in the SAM. A, Quantification of *ZmPIN1a* expression by semiquantitative RT-PCR using total RNA from single normal meristems treated with water or 100 μM kinetin for the indicated times. Expression levels (arbitrary units) were normalized based on ubiquitin expression levels. The 1-h water control levels were adjusted to 100 ($n = 3$; error bars indicate SE). B, Quantification of *ZmPIN1a* by semiquantitative RT-PCR using total RNA from single normal or *abph1* mutant meristems treated with 10 μM kinetin for 4 h. Expression levels (arbitrary units) were normalized based on ubiquitin expression levels. Levels of water control of normal samples were adjusted to 100 ($n = 4$; error bars indicate SE). C, Confocal image of ZmPIN1a-YFP expression in a median longitudinal section through SAM of a seedling treated with control solution for 4 h. D, Confocal image of ZmPIN1a-YFP expression in a median longitudinal section through SAM of a seedling treated with 100 μM kinetin for 4 h. Bars = 100 μm. Additional images are shown in Supplemental Figure S3.

expression was also rapidly up-regulated by cytokinin. Together, these findings suggest that complex cross talk between auxin and cytokinin signaling is involved in the mechanism of phyllotaxy regulation. The reduced PIN expression in *abph1* mutants also suggests an alternative model for the change in phyllotaxy that is observed in these mutants.

DISCUSSION

In this study, we investigated interactions between *ABPH1*-mediated cytokinin signaling and PIN1-dependent polar auxin transport in relation to phyllotaxy. The role of auxin transport by PIN1 and local auxin accumulation in determination of the leaf initiation site and leaf spacing are well established in Arabidopsis and other dicots (Reinhardt et al., 2000, 2003; Heisler et al., 2005; de Reuille et al., 2006; Jonsson et al., 2006; Smith et al., 2006). Polar auxin transport inhibitor studies (Scanlon, 2003) and PIN1 localization (Carraro et al., 2006; this study) strongly suggest that PIN1 also regulates leaf initiation and positioning in monocots such as maize. However, Arabidopsis auxin mutants do not show discrete changes of phyllotactic patterns, and one of the only mutants known to specifically change these patterns is the *abph1* mutant of maize, which is mutated in a cytokinin-inducible response regulator. *ABPH1* is expressed in the P_0, in a region overlapping the domain of PIN1 accumulation. These observations prompted us to investigate interactions between auxin and cytokinin signaling in phyllotaxy.

The interaction between *ABPH1* and auxin signaling was first examined by inhibition of polar auxin transport by NPA. This treatment leads to a loss of leaf initiation, presumably because auxin no longer accumulates at the P_0 (Reinhardt et al., 2000; Scanlon, 2003). We found that NPA treatment of maize shoots for 5 to 10 d resulted in the loss of *ABPH1* expression at the P_0. However, shorter (24 h) treatments did not alter *ABPH1* expression. Thus, the loss of *ABPH1* expression may be a downstream consequence of the loss of leaf initiation in NPA-treated shoot apices, rather than a direct effect. We also tested whether *ABPH1* was auxin inducible and found that it was not (Supplemental Fig. S2). This result is consistent with the hypothesis that *ABPH1* is not a direct target of auxin signaling. Alternatively, *ABPH1* expression might be saturated in normal physiological conditions, where auxin levels are maximal at the P_0 (Reinhardt et al., 2003). Taken together, these results suggest that *ABPH1* expression is dependent on a signal derived from the P_0 but may not be a direct target of polar auxin transport or auxin accumulation. We also consider the possibility that other signal(s), in addition to auxin, may be involved, since the mechanism of NPA action is not specific to auxin (Geldner et al., 2001).

To elucidate interactions between *ABPH1* and the PIN1 polar auxin transporter in maize, we investigated PIN1 expression in wild-type and *abph1* seedling SAMs and embryos. Using a cross-reacting Arabidopsis PIN1 antiserum, we observed a similar PIN1 expression pattern in the maize SAM as found in Arabidopsis. In contrast to a previous report (Carraro et al., 2006), where it was suggested that PIN1 expression in the L1 layer may be less important in maize than in Arabidopsis, we found very clear PIN1 expression in the L1 cells, especially around the P_0. The

polar subcellular localization in these L1 cells and vascular localization patterns of maize PIN1 were similar to those seen in Arabidopsis. PIN1 protein in the L1 was most clearly detected close to the P_0, and not throughout the epidermal layer of the maize SAM, unlike in Arabidopsis, where PIN1 accumulates throughout the L1. However, we suspect that this difference may be due to differences in expression levels between vegetative and inflorescence apices, rather than a fundamental species-specific difference. The published immunolocalization studies of Arabidopsis PIN1 are mostly in inflorescence meristems, and we also observed PIN1 localization throughout the entire L1 layer of inflorescence and floral meristems in maize (Gallavotti et al., 2008). Our observations provide evidence for polar auxin transport in the L1 layer toward the P_0 and its removal through the developing provascular tissue. Hence, it appears likely that polar auxin transport in the L1 and auxin sinks contribute to leaf initiation and spacing in the maize shoot apex, as in Arabidopsis (Reinhardt et al., 2003). Interestingly, we also observed PIN1 expression in the center of the maize SAM by immunolocalization and by expression of the ZmPIN1a-YFP construct. Computer simulations based on PIN1 immunolabeling in Arabidopsis predicted an accumulation of auxin in the central zone, and higher IAA content in this zone has been experimentally confirmed and is proposed to play an important role in creating auxin maxima at incipient leaf initiation sites (de Reuille et al., 2006). Thus, our observations in the maize SAM are consistent with the computational model, even though PIN1 was not detected in the central zone of the Arabidopsis SAM (Reinhardt et al., 2003).

Surprisingly, we found significantly lower PIN1 expression in the P_0 domain of *abph1* seedlings and in the SAM of *abph1* embryos. This difference was not an artifact of genetic background or experimental protocol, because normal PIN1 levels in *abph1* mutants were found later in development, for example in P1 or older leaf primordia, and the PIN1 expression patterns in the scutellums of wild-type and *abph1* embryos were similar. The reduced PIN1 expression in the SAM was confirmed by semiquantitative RT-PCR of a maize PIN1 homolog, suggesting that the regulation of PIN1 at the P_0 by *ABPH1* was at least in part at the transcriptional level.

The positive regulation of *PIN1* by *ABPH1* suggests a new model to explain the larger SAM and altered phyllotaxy phenotypes of *abph1* mutants (Jackson and Hake, 1999; Fig. 7). According to this model, the lower level of *PIN1* expression in the mutants could cause a delay in leaf initiation, allowing for extra growth of the meristem before leaves are initiated. Consistent with this model, we observed that initiation of the first leaf primordia in *abph1* embryos occurs approximately 1 d later than in wild-type siblings (B.-h. Lee, R. Johnston, and D. Jackson, unpublished data). We propose that both the delayed leaf initiation and the enlarged SAM phenotypes contribute to the altered phyllotaxy observed in these mutants (Fig. 7). Given that the formation of auxin maxima is required for leaf initiation, our findings that auxin levels are lower in *abph1* embryos, but that two leaves are initiated simultaneously in these mutants, seem contradictory. However, this may be explained if relative, rather than absolute, auxin levels are required to induce leaf initiation and if leaf initiation is triggered in cells with higher auxin levels relative to their neighbors. This model does not preclude a requirement for a basal auxin threshold for leaf initiation, and in this scenario, leaf initiation would be delayed until the threshold level is reached. There is already evidence for auxin thresholds, for example in vein formation in Arabidopsis flowers, where there is a correlation between *YUCCA* gene dosage and the number of veins formed (Cheng et al., 2006).

Although it is generally thought that type A cytokinin response regulators act as negative regulators or repressors (Hwang and Sheen, 2001), we found that ABPH1 acts as a positive regulator of PIN1 expression. Other examples in which type A cytokinin response regulators act as positive regulators have been described. For example, overexpression of Arabidopsis *ARR4* resulted in increased shoot regeneration in tissue culture (Osakabe et al., 2002) and *ARR* knockouts have reduced *WUS* expression (Leibfried et al.,

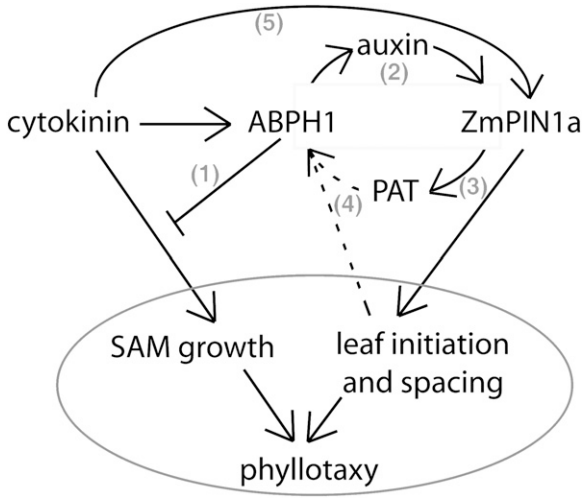

Figure 7. *ABPH1* regulation of both cytokinin and auxin signaling appears to control phyllotaxy in maize. In step 1, *ABPH1* negatively regulates cytokinin induction of SAM growth and therefore functions to maintain normal meristem size. ABPH1 also induces *ZmPIN1a* expression at the P_0, possibly through facilitating auxin accumulation (step 2). *ZmPIN1a* likely functions in polar auxin transport (PAT) in maize to control leaf initiation and spacing (step 3), and PAT, or a downstream event in leaf initiation, is required for *ABPH1* expression, although this effect is probably indirect (dotted lines; step 4). *ZmPIN1a* is also rapidly induced by cytokinin, although this induction appears to be *ABPH1* independent (step 5). We propose that these complex interactions between auxin-mediated leaf initiation/spacing and cytokinin-mediated SAM growth contribute to the regulation of phyllotactic patterns, and our data suggest that ABPH1 performs a central function within this regulatory network.

2005), indicating a positive cytokinin-dependent role in shoot regeneration and *WUS* induction. *ABPH1* is thought to act as a repressor of cytokinin signaling and a negative regulator of SAM size (Giulini et al., 2004). The data presented here indicate that *ABPH1* also acts as a positive regulator of *ZmPIN1a* in the SAM of embryos and seedlings. Consistent with lower *PIN1* expression levels in *abph1*, the mutant embryos also had lower auxin levels. *ABPH1* is specifically expressed in the embryonic SAM (Giulini et al., 2004), so this reduction likely reflects a lower level of auxin in the embryonic SAM. This is supported by our observations of lower ZmPIN1a-YFP expression in the SAM, but not the scutellum, of *abph1* embryos. In Arabidopsis, auxin increases PIN1 levels and facilitates its own efflux, leading to a presumed feed-forward positive reinforcement (Paciorek et al., 2005; Jonsson et al., 2006; Smith et al., 2006). Therefore, *ABPH1* may regulate auxin levels directly, or the effect could be mediated through its positive regulation of PIN1.

Recently, the effects of cytokinins on *PIN* gene expression in Arabidopsis lateral root primordia were also investigated (Laplaze et al., 2007). In contrast to our findings in the shoot meristem, cytokinin treatment blocked the formation of auxin maxima at lateral root initiation sites by down-regulating PIN expression. Although we found the opposite effect, that cytokinin induced PIN1 expression in the shoot meristem, we are confident that our data are consistent. For example, cytokinins induce *ABPH1* expression (Giulini et al., 2004), and ABPH1 is required for PIN1 expression in the P_0. The different effects of cytokinins on PIN1 expression may reflect species-specific differences or, more likely, developmentally specific differences between root (lateral meristem initiation) and shoot (leaf initiation).

In summary, our results provide evidence for both negative and positive regulatory roles of *ABPH1* (Fig. 7). While we cannot be certain that the interactions we found are direct, where we could measure kinetics (e.g. cytokinin induction of *ABPH1* [Giulini et al., 2004] or of PIN1 [reported here]), these effects were rapid, occurring within 1 h, and certainly much faster than the length of a plastochron in maize, which is in the order of 24 h (Smith and Hake, 1992), suggesting that they are likely to be developmentally relevant. Together with the findings of cross talk between cytokinin and auxin signaling in initiation and regulation of the Arabidopsis root apical meristem or of lateral root primordia (Dello Ioio et al., 2007; Laplaze et al., 2007; Müller and Sheen, 2008), our results suggest a common theme of auxin-cytokinin cross talk in the regulation of plant apical meristems and organ initiation.

MATERIALS AND METHODS

Plant Treatments

For NPA treatment of cultured apices, we followed published methods (Scanlon, 2003). Briefly, shoot apices from 2-week-old maize (*Zea mays*) seedlings were dissected down to the SAM with four to five leaves attached and placed on MS/phytagel (Sigma) medium with or without 30 μM NPA (Chem Service).

For hormone and NPA treatments, 2-week-old maize seedlings were cut at the root-shoot junction and the shoot portion was placed in solution as described by Giulini et al. (2004). Kinetin or IAA was dissolved in 1 M KOH to make 10 mM stock solutions. The working solutions were diluted from the stock, and the pH was adjusted to 5.8 with HCl. The control solution was prepared from the same volume of 1 M KOH diluted with water, and pH for the control was also adjusted. NPA was dissolved in dimethyl sulfoxide and then diluted with water to make a 30 μM solution. A control solution was made by adding an equivalent quantity of dimethyl sulfoxide to water. After appropriate treatments, meristems were dissected and collected for further analyses.

In Situ Hybridization and Immunolocalization

Using the full-length cDNA of *ABPH1*, in situ hybridization was carried out on shoot apices following the method described by Jackson et al. (1994).

For immunolocalization, 2-week-old maize shoot apices were fixed in 5% acetic acid, 45% ethanol, and 10% formalin overnight. After dehydration through an ethanol series, the apices were infiltrated with Steedman's wax (polyethylene glycol 400 distearate:hexadecanol, 9:1) at 37°C (Steedman, 1957). Following embedding and sectioning, 10-μm sections were placed onto Chrom-Alum-coated slides (0.5% fish gelatin [Sigma] and 0.05% chromium potassium sulfate). For antibody reactions, Steedman's wax was removed in 100% ethanol. The sections were then rehydrated in an ethanol series and blocked by incubating in phosphate-buffered saline (PBS) buffer (130 mM NaCl and 10 mM PO_4) with 1% bovine serum albumin. The slides were incubated with an Arabidopsis (*Arabidopsis thaliana*) PIN1 antiserum (Boutte et al., 2006; 1:300 dilution) in PBS with 1% bovine serum albumin for 2 h at room temperature. After two to three washes in PBS with 1% fish gelatin, the slides were incubated with a Cy3-conjugated anti-rabbit secondary antibody (1:800 dilution; Jackson ImmunoResearch Laboratory). Slides were washed five times in PBS with 1% fish gelatin, mounted in Citifluor AF1 (Electron Microscopy Sciences), and observed by fluorescence microscopy.

Molecular Biology

The ZmPIN1a-YFP construct has been described (Gallavotti et al., 2008). The ABPH1-RFP construct was generated using the fluorescent tagging of full-length proteins method (Tian et al., 2004). The construct includes 5′ upstream DNA sequence (3,558 bp) and 3′ downstream sequence (662 bp) of the *ABPH1* open reading frame (842 bp) with a monomeric RFP (Campbell et al., 2002) internally inserted between nucleotides 830 and 831 of the *ABPH1* open reading frame. This causes internal insertion of RFP between amino acids 132 and 133 of the ABPH1 protein. The primers used were AB1-P3.5F-P1 (5′-gctcgatccacctaggctCAGGGTGCCAAGATCTCTCC-3′), AB1-RFP-P2 (5′-tccacctccacctccaggccggccGCGGCTGCACAGGCGCGA-3′), AB1-RFP-P3 (5′-tggtgctgctgcggccgctggggccGTCCTGCGGTGAGCACGG-3′), and AB1-P4 (5′-cgtagcgagaccacaggaGCAACCGTGACCAAGATGAG-3′). Gene-specific sequences are shown in uppercase letters. Following the fluorescent tagging of full-length protein method, the fusion product was subcloned into the pTF101.1-derived pAM1006 vector containing a Gateway cassette.

For analysis of *ZmPIN1a* by semiquantitative RT-PCR, maize shoot meristems were isolated from 2-week-old normal and *abph1* maize plants. Total RNA was extracted with Trizol (Invitrogen). Semiquantitative RT-PCR was carried out for *ZmPIN1a* using the One-Step RT-PCR kit (Qiagen) with primers UCSD-ZmPIN1-F1 (5′-ATAATCGCGTGCGGGAACAA-3′) and UCSD-ZmPIN1-R1 (5′-TCCTGCTCCACATCCCCATC-3′) and for ubiquitin with primers Ubi 5′ (5′-TAAGCTGCCGATGTGCCTGCGTCG-3′) and Ubi 3′ (5′-CTGAAAGACAGAACATAATGAGCACAG-3′). The ubiquitin gene was chosen as a loading control. The one-step RT-PCR was done as follows: 50°C for 30 min, 94°C for 15 min, seven cycles of 94°C for 15 s, 65°C (−1°C per cycle) for 15 s, and 72°C 20 s, and 18 cycles of 94°C for 15 s, 59°C for 15 s, and 72°C for 20 s. For analysis of *ABPH1* expression by semiquantitative RT-PCR following NPA treatment, the SAM plus two leaf primordia were dissected from seedlings treated for 24 h with NPA or control solution. Two biological replicates were used for each treatment, and 10 SAMs were pooled for each replicate. Total RNA was extracted using Trizol, followed by RNAeasy columns (Qiagen). Semiquantitative RT-PCR was carried out using the SuperScript III One-Step RT-PCR kit (Invitrogen). PCR cycles were as follows: 94°C for 4 min, 10 cycles of 94°C for 30 s, 65°C (−1°C per cycle) for 20 s, and 75°C

for 20 s, and 26 cycles of 94°C for 30 s, 55°C for 20 s, and 72°C for 30 s. The *ABPH1* primer sequences were Fwd (5′-GATGGCGAGCCGCAAGTGT-3′) and Rev (5′-AATGCCGCTGCTACAGCTACCA-3′; Giulini et al., 2004). Ubiquitin was used as a loading control. After fractionation on a 1.2% agarose gel, the band intensity was quantified using a GelDoc system (Bio-Rad) by ethidium bromide fluorescence or a phosphoimager (Fuji) after DNA blot hybridization. Semiquantitative RT-PCR was performed using a cycle number low enough to ensure that amplification was in the linear phase. *ZmPIN1a* and *ABPH1* signal levels were normalized by the ubiquitin signal intensity.

Protein Blot Analysis

Proteins were extracted from maize shoot apices by grinding in the protein extraction buffer (150 mM NaCl, 50 mM Tris-Cl [pH 7.5], 1 mM phenylmethylsulfonyl fluoride, 0.5 mM dithiothreitol, and Complete EDTA-free Protease Inhibitor Cocktail; Roche Applied Science).

The total fraction was obtained after centrifugation of the sample at 8,000*g* at 4°C for 10 min. This total fraction was centrifuged at 100,000*g* at 4°C for 1 h to separate soluble and membrane fractions; the supernatant fluid was taken as the soluble fraction, and the pellet was resuspended in extraction buffer containing 1% Triton X-100, incubated on ice for 30 min, and centrifuged at 100,000*g* at 4°C for 1 h. The resulting supernatant fluid was the membrane fraction. SDS-polyacrylamide gels (8%) were loaded with 16 μg of protein per lane. After running at 200 V for 45 min, they were blotted onto a polyvinylidene fluoride membrane (Millipore) using a Trans-Blot SD semidry transfer cell (Bio-Rad). Blocking was carried out by immersing the membrane in 5% nonfat milk in TBS-T buffer (140 mM NaCl, 20 mM Tris, pH 7.6, and 0.1% [v/v] Tween 20) for 1 h. The Arabidopsis PIN1 antiserum was diluted in the blocking solution to 1:2,000 and incubated with the blocked membrane for 1 h. After washing three times with TBS-T for 10 min, a horseradish peroxidase-labeled anti-mouse antibody (Amersham Bioscience) was diluted in the blocking solution to 1:5,000 and used as a secondary antibody. After 1 h of incubation, the membrane was washed four times for 10 min with TBS-T, visualized by the ECL Plus Western Blotting Detection System (Amersham Bioscience), and exposed to x-ray films for 30 s.

3D Image Reconstructions

A series of PIN1 immunolocalization images was collected using fluorescence microscopy from sequential sections of normal and *abph1* SAMs (11 10-μm sections for normal SAM; 18 10-μm sections for *abph1* SAM). Each series was used to construct 3D images following three steps: (1) preprocessing of the images in order to identify the areas of interest (Costa and Cesar, 2000) and to align each subsequent pair of slices; (2) morphing between subsequent pairs of images in order to obtain smoother transitions between slices, using Squrlz Morph application (http://www.xiberpix.com/SqirlzMorph.html); and (3) 3D reconstruction, using the whole set of images, of the structures of interest (Schroeder et al., 2003). Finally, the data were exported into Virtual Reality Modeling Language format.

Hormone Content Analysis

To achieve similar developmental stages with isogenic controls, pollen from normal maize or *abph1* mutants was used to pollinate ears of *abph1* mutants, generating *abph1* heterozygous ("wild type") and homozygous embryos, respectively. Embryos were harvested at about 10 d after pollination. For each extraction, 10 embryos (7–10 mg fresh weight) were harvested and soaked in 1 mL of extraction solvent (methanol:chloroform:water, 3:1:1). Hormones and related compounds were extracted using a TissueLyser (Qiagen) with zirconia beads, an HLB column (Waters), and an MCX column (Waters). In the solid-phase extraction, the cytokinin nucleotides were eluted with 0.35 M NH_4OH, other cytokinin species were eluted with 0.35 M NH_4OH in 60% methanol, and the auxins were eluted with methanol (Dobrev and Kaminek, 2002). The cytokinins were then measured with a liquid chromatography-mass chromatography system (UPLC/Quattro Ultima Pt; Waters) as described previously (Dobrev and Kaminek, 2002; Nakagawa et al., 2005). For measurement of IAA and IAAsp, the fraction eluted from the MCX column (Dobrev and Kaminek, 2002) was further purified using DEAE-cellulose. IAA and the amino acid conjugates were eluted with 0.5% and 3% formic acid, respectively. As the internal standards, stable isotope IAA (deuterium-labeled [$^2H_5$]IAA; OlchemIm) was added together with the internal standard of cytokinins. The recovery yield of IAAsp was calculated using that of IAA. The IAA and IAAsp were determined with a liquid chromatography-mass chromatography system. Cone voltage for detection of IAA and IAAsp was 53 V, collision energy was 13 to 19 eV, and capillary voltage was 3.12 kV.

Confocal Imaging of ZmPIN1a-YFP and ABPH1-RFP Expression in Embryos

Confocal images were taken with a Zeiss LSM510 confocal microscope, and images were acquired using the LSM software. For analysis of ZmPIN1a-YFP expression, wild-type (B73) and *abph1* ears were pollinated with pollen from *abph1* plants expressing the *ZmPIN1a-YFP* construct to generate normal and *abph1* embryos, respectively. For colocalization of ZmPIN1a-YFP and ABPH1-RFP, pollen from plants expressing both constructs was used to pollinate wild-type ears. Embryos were dissected from kernels at 11 to 14 d after pollination, fixed for 10 min in 2.5% paraformaldehyde, mounted on glass microscope slides in FocusClear (CelExplorer Labs), and left to clear for 30 min.

Quantification of ZmPIN1a-YFP after Cytokinin Treatment

Seedlings expressing the ZmPIN1a-YFP construct were treated for 4 h with 100 μM kinetin or control solution. Median longitudinal hand sections were made of seedling apices and then mounted on glass microscope slides in 1× PBS buffer. Confocal settings were optimized so that fluorescence levels were below saturation and no fluorescence was seen in control (nonexpressing) SAMs. Quantification of fluorescence was done using ImageJ software (http://rsb.info.nih.gov/ij). For each section, the P_0 site of leaf initiation, marked by high PIN1-YFP expression, was outlined using the polygon tool. Mean fluorescence intensity (on a scale of 0–255) and the area of the P_0 were calculated for the selected region. Integrated density was calculated by multiplying the mean fluorescence intensity by the area. Mean fluorescence intensity was also quantified for a square with a set area of 225 μm^2 (15 μm × 15 μm) that was centered on the P_0 leaf primordium of each sample. The values obtained were compared using Student's *t* test.

Supplemental Data

The following materials are available in the online version of this article.

Supplemental Figure S1. Maize PIN1 is detected by an *Arabidopsis* PIN1 antiserum.

Supplemental Figure S2. *ABPH1* is not induced by auxin.

Supplemental Figure S3. Cytokinin treatment induces ZmPIN1a-YFP in the P_0 leaf primordium.

Supplemental Table S1. Contents of cytokinins, auxin, and related compounds in normal and *abph1* embryos.

Supplemental Table S2. Quantification of ZmPIN1a-YFP fluorescence in the SAM of kinetin-treated and control seedlings.

Supplemental Video S1. 3D reconstruction of maize PIN1 immunolocalization in the shoot apex of normal maize.

Supplemental Video S2. 3D reconstruction of maize PIN1 immunolocalization in the shoot apex of *abph1*.

ACKNOWLEDGMENTS

We thank Amitabh Mohanty for technical advice in ZmPIN1a-YFP and ABPH1-RFP construction, Tim Mulligan for plant care, Erin Jimenez for assistance with dissections and RT-PCR, and members of the Jackson laboratory for valuable advice.

Received February 12, 2009; accepted March 19, 2009; published March 25, 2009.

LITERATURE CITED

Barlier I, Kowalczyk M, Marchant A, Ljung K, Bhalerao R, Bennett M, Sandberg G, Bellini C (2000) The SUR2 gene of Arabidopsis thaliana

encodes the cytochrome P450CYP83B1, a modulator of auxin homeostasis. Proc Natl Acad Sci USA **97:** 14819–14824

Barratt NM, Dong WQ, Gage DA, Magnus V, Town CD (1999) Metabolism of exogenous auxin by Arabidopsis thaliana: identification of the conjugate N-alpha-(indol-3-ylacetyl)-glutamine and initiation of a mutant screen. Physiol Plant **105:** 207–217

Benkova E, Michniewicz M, Sauer M, Teichmann T, Seifertova D, Jurgens G, Friml J (2003) Local, efflux-dependent auxin gradients as a common module for plant organ formation. Cell **115:** 591–602

Boutte Y, Crosnier MT, Carraro N, Traas J, Satiat-Jeunemaitre B (2006) The plasma membrane recycling pathway and cell polarity in plants: studies on PIN proteins. J Cell Sci **119:** 1255–1265

Brand U, Fletcher JC, Hobe M, Meyerowitz EM, Simon R (2000) Dependence of stem cell fate in Arabidopsis and a feedback loop regulated by CLV3 activity. Science **289:** 617–619

Campbell RE, Tour O, Palmer AE, Steinbach PA, Baird GS, Zacharias DA, Tsien RY (2002) A monomeric red fluorescent protein. Proc Natl Acad Sci USA **99:** 7877–7882

Carraro N, Forestan C, Canova S, Traas J, Varotto S (2006) ZmPIN1a and ZmPIN1b encode two novel putative candidates for polar auxin transport and plant architecture determination of maize. Plant Physiol **142:** 254–264

Cheng YF, Dai XH, Zhao YD (2006) Auxin biosynthesis by the YUCCA flavin monooxygenases controls the formation of floral organs and vascular tissues in Arabidopsis. Genes Dev **20:** 1790–1799

Costa LDF, Cesar RM Jr (2000) Shape Analysis and Classification: Theory and Practice. CRC Press, Boca Raton, FL

Dello Ioio R, Linhares FS, Scacchi E, Casamitjana-Martinez E, Heidstra R, Costantino P, Sabatini S (2007) Cytokinins determine *Arabidopsis* root meristem size by controlling cell differentiation. Curr Biol **17:** 678–682

de Reuille PB, Bohn-Courseau I, Ljung K, Morin H, Carraro N, Godin C, Traas J (2006) Computer simulations reveal properties of the cell-cell signaling network at the shoot apex in Arabidopsis. Proc Natl Acad Sci USA **103:** 1627–1632

Dobrev PI, Kaminek M (2002) Fast and efficient separation of cytokinins from auxin and abscisic acid and their purification using mixed-mode solid-phase extraction. J Chromatogr A **950:** 21–29

Gallavotti A, Yang Y, Schmidt RJ, Jackson D (2008) The relationship between auxin transport and maize branching. Plant Physiol **147:** 1913–1923

Geldner N, Friml J, Stierhof YD, Jurgens G, Palme K (2001) Auxin transport inhibitors block PIN1 cycling and vesicle trafficking. Nature **413:** 425–428

Giulini A, Wang J, Jackson D (2004) Control of phyllotaxy by the cytokinin-inducible response regulator homologue *ABPHYL1*. Nature **430:** 1031–1034

Heisler MG, Ohno C, Das P, Sieber P, Reddy GV, Long JA, Meyerowitz EM (2005) Patterns of auxin transport and gene expression during primordium development revealed by live imaging of the Arabidopsis inflorescence meristem. Curr Biol **15:** 1899–1911

Higuchi M, Pischke MS, Mahonen AP, Miyawaki K, Hashimoto Y, Seki M, Kobayashi M, Shinozaki K, Kato T, Tabata S, et al (2004) In planta functions of the Arabidopsis cytokinin receptor family. Proc Natl Acad Sci USA **101:** 8821–8826

Hwang I, Sheen J (2001) Two-component circuitry in Arabidopsis cytokinin signal transduction. Nature **413:** 383–389

Jackson D, Hake S (1999) Control of phyllotaxy in maize by the abphyl1 gene. Development **126:** 315–323

Jackson D, Veit B, Hake S (1994) Expression of maize Knotted1-related homeobox genes in the shoot apical meristem predicts patterns of morphogenesis in the vegetative shoot. Development **120:** 405–413

Jonsson H, Heisler MG, Shapiro BE, Meyerowitz EM, Mjolsness E (2006) An auxin-driven polarized transport model for phyllotaxis. Proc Natl Acad Sci USA **103:** 1633–1638

Laplaze L, Benkova E, Casimiro I, Maes L, Vanneste S, Swarup R, Weijers D, Calvo V, Parizot B, Herrera-Rodriguez MB, et al (2007) Cytokinins act directly on lateral root founder cells to inhibit root initiation. Plant Cell **19:** 3889–3900

Laux T (2003) The stem cell concept in plants: a matter of debate. Cell **113:** 281–283

Leibfried A, To JPC, Busch W, Stehling S, Kehle A, Demar M, Kieber JJ, Lohmann JU (2005) WUSCHEL controls meristem function by direct regulation of cytokinin-inducible response regulators. Nature **438:** 1172–1175

Müller B, Sheen J (2008) Cytokinin and auxin interaction in root stem-cell specification during early embryogenesis. Nature **453:** 1094–1097

Nakagawa H, Jiang CJ, Sakakibara H, Kojima M, Honda I, Ajisaka H, Nishijima T, Koshioka M, Homma T, Mander LN, et al (2005) Overexpression of a petunia zinc-finger gene alters cytokinin metabolism and plant forms. Plant J **41:** 512–523

Nishimura C, Ohashi Y, Sato S, Kato T, Tabata S, Ueguchi C (2004) Histidine kinase homologs that act as cytokinin receptors possess overlapping functions in the regulation of shoot and root growth in *Arabidopsis*. Plant Cell **16:** 1365–1377

Okada K, Ueda J, Komaki MK, Bell CJ, Shimura Y (1991) Requirement of the auxin polar transport system in early stages of *Arabidopsis* floral bud formation. Plant Cell **3:** 677–684

Osakabe Y, Miyata S, Urao T, Seki M, Shinozaki K, Yamaguchi-Shinozaki K (2002) Overexpression of Arabidopsis response regulators, ARR4/ATRR1/IBC7 and ARR8/ATRR3, alters cytokinin responses differentially in the shoot and in callus formation. Biochem Biophys Res Commun **293:** 806–815

Ostin A, Kowalyczk M, Bhalerao RP, Sandberg G (1998) Metabolism of indole-3-acetic acid in Arabidopsis. Plant Physiol **118:** 285–296

Paciorek T, Zazimalova E, Ruthardt N, Petrasek J, Stierhof YD, Kleine-Vehn J, Morris DA, Emans N, Jurgens G, Geldner N, et al (2005) Auxin inhibits endocytosis and promotes its own efflux from cells. Nature **435:** 1251–1256

Petrasek J, Mravec J, Bouchard R, Blakeslee JJ, Abas M, Seifertova D, Wisniewska J, Tadele Z, Kubes M, Covanova M, et al (2006) PIN proteins perform a rate-limiting function in cellular auxin efflux. Science **312:** 914–918

Reinhardt D, Mandel T, Kuhlemeier C (2000) Auxin regulates the initiation and radial position of plant lateral organs. Plant Cell **12:** 507–518

Reinhardt D, Pesce ER, Stieger P, Mandel T, Baltensperger K, Bennett M, Traas J, Friml J, Kuhlemeier C (2003) Regulation of phyllotaxis by polar auxin transport. Nature **426:** 255–260

Rupp HM, Frank M, Werner T, Strnad M, Schmulling T (1999) Increased steady state mRNA levels of the STM and KNAT1 homeobox genes in cytokinin overproducing Arabidopsis thaliana indicate a role for cytokinins in the shoot apical meristem. Plant J **18:** 557–563

Scanlon MJ (2003) The polar auxin transport inhibitor N-1-naphthylphthalamic acid disrupts leaf initiation, KNOX protein regulation, and formation of leaf margins in maize. Plant Physiol **133:** 597–605

Schoof H, Lenhard M, Haecker A, Mayer KFX, Jurgens G, Laux T (2000) The stem cell population of Arabidopsis shoot meristems is maintained by a regulatory loop between the CLAVATA and WUSCHEL genes. Cell **100:** 635–644

Schroeder WJ, Martin KM, Lorensen WE (2003) The Visualization Toolkit: An Object-Oriented Approach to 3D Graphics, Ed 3. Kitware, New York

Skoog F, Miller CO (1957) Chemical regulation of growth and organ formation in plant tissues cultured *in vitro*. Symp Soc Exp Biol **11:** 118–130

Smith LG, Hake S (1992) The initiation and determination of leaves. Plant Cell **4:** 1017–1027

Smith RS, Guyomarc'h S, Mandel T, Reinhardt D, Kuhlemeier C, Prusinkiewicz P (2006) A plausible model of phyllotaxis. Proc Natl Acad Sci USA **103:** 1301–1306

Spradling A, Drummond-Barbosa D, Kai T (2001) Stem cells find their niche. Nature **414:** 98–104

Steedman HF (1957) Polyester wax: a new ribboning embedding medium for histology. Nature **179:** 1345

Tian GW, Mohanty A, Chary SN, Li SJ, Paap B, Drakakaki G, Kopec CD, Li JX, Ehrhardt D, Jackson D, et al (2004) High-throughput fluorescent tagging of full-length Arabidopsis gene products in planta. Plant Physiol **135:** 25–38

Weigel D, Jurgens G (2002) Stem cells that make stems. Nature **415:** 751–754

Werner T, Motyka V, Laucou V, Smets R, Van Onckelen H, Schmulling T (2003) Cytokinin-deficient transgenic *Arabidopsis* plants show multiple developmental alterations indicating opposite functions of cytokinins in the regulation of shoot and root meristem activity. Plant Cell **15:** 2532–2550

Werner T, Motyka V, Strnad M, Schmulling T (2001) Regulation of plant growth by cytokinin. Proc Natl Acad Sci USA **98:** 10487–10492

Wisniewska J, Xu J, Seifertova D, Brewer PB, Ruzicka K, Blilou I, Rouquie D, Benkova E, Scheres B, Friml J (2006) Polar PIN localization directs auxin flow in plants. Science **312:** 883